Journal of Korean Association of Crystal Growth
Vol. 10, No. 1 (2000) 1-4

Surface analysis of a-Si_xC_{1-x}: H deposited by RF plasma-enhanced CVD

Yong-Tak Kim, Woo-Seok Yang, Hyun Lee, Byungyou Hong* and Dae-Ho Yoon

School of Metallurgical and Materials Engineering, Sungkyunkwan University, Suwon 440-746, Korea
**School of Electrical and Computer Engineering, Sungkyunkwan University, Suwon 440-746, Korea*

(Received June 6, 1999)

Abstract Thin films of hydrogenated amorphous silicon carbide compounds (a-Si_xC_{1-x}: H) of different compositions were deposited on Si substrate by RF plasma-enhanced chemical vapor deposition (PECVD). Experiments were carried out using silane (SiH_4) and methane (CH_4) as the gas precursors at 1 Torr and at a low substrate temperature (250°C). The gas flow rate was changed with the other parameters (pressure, temperature, RF power) fixed. The substrate was Si(100) wafer and all of the films obtained were amorphous. The bonding structure of a-Si_xC_{1-x}: H films deposited was investigated by X-ray photoelectron spectroscopy (XPS) for the film compositions. In addition, the surface morphology of films was investigated by atomic force microscopy (AFM).

1. Introduction

The hydrogenated amorphous silicon carbide (a-Si_xC_{1-x}: H) films have the useful property that the silicon content can be changed by various conditions, especially the ratio of silane and methane. The hydrogenated amorphous silicon carbide (a-Si_xC_{1-x}: H) and hydrogenated amorphous silicon (a-Si : H) are important materials for optoelectronic devices such as solar cells [1-5]. a-Si_xC_{1-x}: H film attracted attention in recent years because the film is superior to a-Si : H in term of its thermal and photo-stabillities, and its optical and electrical properties can be varied readily by adjusting the process parameter. The device applications of a-Si_xC_{1-x}: H film introduce light-emitting diodes [6], phototransistors [7], photodetectors [8, 9] and solar collectors [10]. The films has also been used as wear-resistant coating [11] and X-ray lithography masks [12, 13]. It is known that the band gap of a-Si_xC_{1-x}: H films grown by PECVD can be varied over 1.9~3.2 eV by controlling the silicon content in the film.

In this work, a-Si_xC_{1-x}: H films which have different compositions were prepared and the sample properties with the compositions of a-Si_xC_{1-x}: H films was investigated. The deposited samples have been analyzed by XPS and AFM. In particular, the XPS measurements have been utilized to analyze the core-level electrons.

2. Experimental procedure

a-Si_xC_{1-x}: H films were deposited by PECVD technique, from appropriated gaseous mixtures of silane (SiH_4) and methane (CH_4). A schematic of the PECVD equipment is shown in Fig. 1. The reaction system is of the parallel planar discharge type using a rectangular RF electrode (lower) and substrate electrode (upper). The substrate is set on the tray with the surface to be coated facing downward, so that deposition of dust particles and flakes can be minimized. The n-type Si wafers in (100) orientation were used as the substrate. Prior to film deposition, the wafer was dipped in a 10 % hydrofluoric acid for about 40 s, rinsed in deionized water and acetone, and finally dried in a nitrogen ambient. The base pressure of the chamber is 4×10^{-5} Torr and the source gas was SiH_4 (10 % dilution in N_2) and CH_4. A typical RF (13.56 MHz) input power was 150 W. The substrate temperature was kept at 250°C, and the pressure during deposition was 1 Torr. The silane gas flow rate (x) was changed from the ratio of 0.35 to 0.66 standard cubic

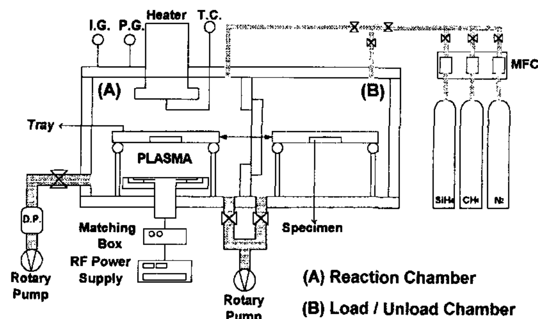

Fig. 1. A schematic of the RF PECVD equipment.

centimeter per minute (sccm) in a-Si_xC_{1-x}: H.

The XPS measurement was run on a Perkin-Elmer PHI 5700 surface analysis instrument using Mg K_α X-rays (1253.6 eV) as the photoexcitation source with an electron take-off angle of 45° from the surface normal.

The morphology of film surface was examined by AFM using the contact mode. In the contact mode, controlling the distance maintains the force exerted by the cantilever on the surface. For a scanning speed of 1~2 s/line, a surface image consisting of 256 lines requires a time of about 5 min.

3. Results and discussion

3.1. XPS measurement

The systematic XPS analysis has been performed on a-Si_xC_{1-x}: H compounds, which are expected to have a rate of compositions within each sample. The photoemission measurement has been performed on a series of samples before and after removing the surface oxide layer. After the Ar sputter cleaning treatment, oxygen was found to be still present in samples. A curve fitting with mixed Gaussian/Lorentzian functions was performed on smoothed data. The energy peak positions used in the analysis of XPS results are well known in papers published previously [14-16]. A detailed analysis of the C1s core level electron is helpful in evaluating the variations of the compound compositions and the oxidation degree of unstable films, as shown in Fig. 2. The C1s peak was able to be fitted by C-O-H, C-C, C=O and C-Si contribution. The spectrum of Fig. 2(a) and (b) occur due to the charge transfer resulting from the increase of the average electronegativity of the surroundings [17]. The charging effect and C-Si peak disappearance were observed for specimen with much oxidation as all of peak energy were shifted. It was observed the shift in the binding energy of compositions depending on the change in an oxidation state. The highly oxidized samples have higher binding energies, and emit electrons with lower kinetic energies. No charging effect was observed in the Fig. 2(c) and (d). The intensity of C-Si peak decreases with increasing carbon contents because the electronegativity of carbon is higher than that of silicon. The intensity of C-C bonds increases with decreasing C-Si bonds in C1s peak. Figure 2(c) and (d) samples showed a single peak around 283 eV with a small shoulder at 284 eV, indicating that the

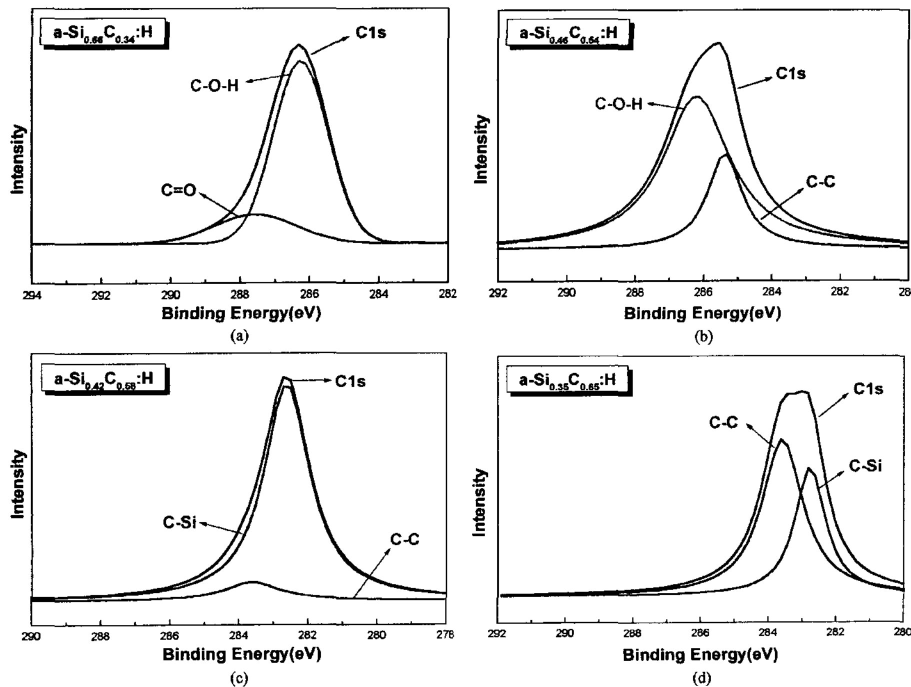

Fig. 2. XPS core level spectra in the C1s binding energy region for samples after Ar sputter cleaning treatment; (a) a-$Si_{0.66}C_{0.34}$: H (b) a-$Si_{0.46}C_{0.54}$: H, (c) a-$Si_{0.42}C_{0.58}$: H, (d) a-$Si_{0.35}C_{0.65}$: H.

Table 1
The XPS results for a-Si_xC_{1-x}: H films prepared under different gas flow rate

	C-Si (%)	C-C (%)	C-O-H (%)	C=O (%)
a-$Si_{0.66}C_{0.34}$: H	-	-	81.1	18.9
a-$Si_{0.46}C_{0.54}$: H	-	-	75.6	24.4
a-$Si_{0.42}C_{0.58}$: H	90.8	9.2	-	-
a-$Si_{0.35}C_{0.65}$: H	35.3	64.7	-	-

films have both C-Si bonds (~282.7 eV) and C-C bonds (~283.6 eV) [18].

The composition of the four samples obtained from the XPS experiments are listed in Table 1. The remarkable decrease in C-Si from 90.8 % to 35.3 %, as silane is decreased from 0.42 to 0.35 sccm is interesting to note. We consider that when SiH_4 is decomposed efficiently by the RF plasma, SiH_3 radicals, which are thought to be the main precursors for a-Si_xC_{1-x}: H deposition, are generated and they have an effect of making C-Si bonds in the films.

3.2. AFM measurement

Atomically sharp tip interacting with a surface scans the surface features to produce an image [19]. The tip is usually attached to a small cantilever and used in the contact mode. Typical AFM images of the surface of a-Si_xC_{1-x}: H films are shown in Fig. 3(a)-(d), respectively. Note that the surface is covered with islands of different sizes. Such a microstructure is observed in all fabricated samples while the concentration and the size of islands depend on the deposition condition. At the same time, from the result of the diffraction analysis we could not detect microcrystals in any samples. The nature of these islands on the surface was clarified using the combined analysis of height and phase images obtained by AFM. We calculated height and diameter for all types of islands on the surface of $4 \times 4\ \mu m^2$.

Samples for Fig. 3(c) and (d) show a lower value of surface roughness as compared to samples for Fig. 3(a) and (b) with a charging effect. We confirmed the relation of charging effect and surface roughness. The surface roughness for a-$Si_{0.66}C_{0.34}$: H, a-$Si_{0.46}C_{0.54}$: H, a-$Si_{0.42}C_{0.58}$: H, and a-$Si_{0.35}C_{0.65}$: H are 1.59, 1.51, 0.92, and 0.99 Å, respectively. We controlled surface reaction by precursor species regulation. Precursor species regulation was realized by gas flow control. These images indicate that gas flow control has effect on surface morphology. Figure 3(c) of a-$Si_{0.42}C_{0.58}$: H shows the lowest value of roughness. The optimum deposition conditions for the surface roughness are : plasma pressure 1 Torr; electrode distance 15.6 mm; total gas flows in the range 20~50 sccm; substrate temperature 250°C; rf power 150 W. This reduction of the surface roughness at a-$Si_{0.42}C_{0.58}$: H is expected to contribute to improving the *p/i* interface in a *p-i-n* solar cell. Later, we will report the relationship of the oxygen contents and the charging effect.

4. Summary

a-Si_xC_{1-x}: H compounds produced by PECVD technique from SiH_4+CH_4 gas mixtures have been investigated as a function of the compositional gas ratio.

1) Specimen with much oxidation was observed to

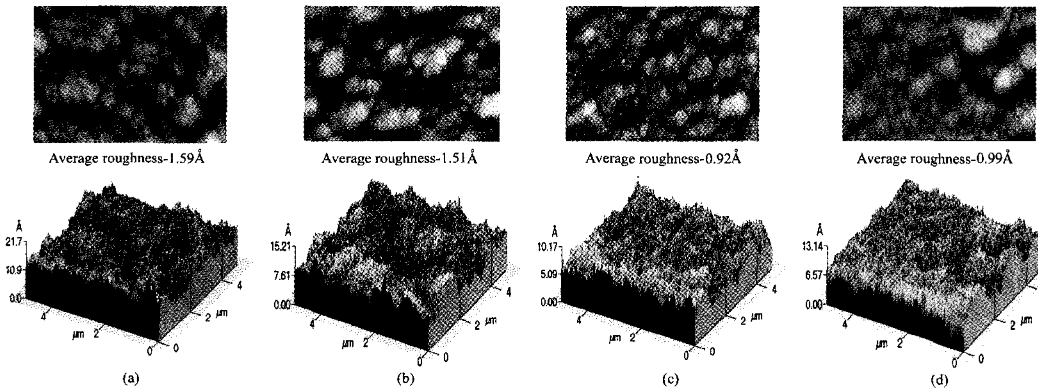

Fig. 3. AFM images the surface of a-Si_xC_{1-x}: H films; (a) a-$Si_{0.66}C_{0.34}$: H, (b) a-$Si_{0.46}C_{0.54}$: H, (c) a-$Si_{0.42}C_{0.58}$: H, (d)a-$Si_{0.35}C_{0.65}$: H.

have a charging effect because a shift of energy for C-Si peak disappeared. There will be small shifts with the charging effect in the binding energy due to changes in an oxidation state. The energy of C-Si peak increased with the decreasing silicon contents.

2) We controlled surface reaction by precursor species regulation. Precursor species regulation was realized by gas flow control. These images indicate that gas flow control has effect on surface morphology. Figure 3(c) of a-$Si_{0.42}C_{0.58}$:H shows the lowest value of roughness.

Acknowledgments

The authors wish to thank Samsung Advanced Institute of Technology for the donation of PECVD equipment (ULVAC CPD-6018).

References

[1] A. anderson and W.E. Spear, Phil. Mag. 35 (1977) 1.
[2] R.S. Sussmann and R. Ogden, Phil. Mag. 44 (1981) 137.
[3] J. Bullot, M. Gauthier, M. Schmidt, Y. Catherine and Y. Zamouche, Phil. Mag. 49 (1984) 489.
[4] J. Sotiropoulos and G. Weiser, J. Non-Cryst. Solids 92 (1987) 95.
[5] J.I. Pankove, Hydrogenated Amorphous Silicon. Part D, Device Application (Academic, New York, 1984).
[6] W. Hong, N.F. Shin, T.S. Jen, S.L. Ning and C.Y. Chang, IEEE. Electron Device Lett. 13 (1992) 375.
[7] T. Wu, Y.K. Fang, J.W. Hing and C.Y. Chang, Solid-State Electron. 34 (1991) 189.
[8] K. Dutta, M. Morosawa and Y. Hatanaku, Solid-State Electron. 35 (1992) 1483.
[9] K. Fang, S.B. Hwang, K.H. Chen, C.R. Liu, M.J. Tsai and L.C. Kuo, IEEE Trans. Electron Devices 39 (1992) 292.
[10] Y. Tawada, K. Tsuge, M. Kondo, H. Okamoto and Y. Hamakawa, J. Appl. Phys. 53 (1982) 5273.
[11] W. Zhang, M. Lelogeais and M. Ducarroir, Jpn. J. Appl. Phys. 31 (1992) 4053.
[12] H. Windischmann, J. Vac. Sci. Technol. 9 (1991) 2459.
[13] A. Jean, M. Chaker, Y. DiaWara, P.K. Leung, E. Gat, P.P. Mereier, H. Pepin, S. Gujrathi, G.G. Ross and J.C. Kieffer, J. Appl. Phys. 72 (1992) 3110.
[14] W.K. Choi, T.Y. Ong and L.S. Tan, J. Appl. Phys. 83 (1998) 4968.
[15] W.K. Choi, F.L. Loo, C.H. Ling, F.C. Loh and K.L. Tan, J. Appl. Phys. 78 (1995) 7289.
[16] S.E. Hicks, A.G. Fitzgerald, S.H. Baker and T.J. Dines, Philos. Mag. B 62 (1990) 193.
[17] D.V. Tsu and G. Lucovsky, J. Non-Cryst. Solid 97/98 (1987) 839.
[18] F. Tadashi, Y. Masahiro, F. Takashi and M. Hiroyuki, Jpn. J. Appl. Phys. 36 (1997) 280.
[19] D. Sarid, Scanning force microscopy (Oxford University Press, Oxford, 1994).